

Mirror nuclei constraint in mass formula

Ning Wang,^{1,*} Zuoying Liang,¹ Min Liu,^{1,2} and Xizhen Wu³

¹*Department of Physics, Guangxi Normal University, Guilin 541004, P. R. China*

²*College of Nuclear Science and Technology,*

Beijing Normal University, Beijing, 100875, P. R. China

³*China Institute of Atomic Energy, Beijing 102413, P. R. China*

Abstract

The macroscopic-microscopic mass formula is further improved by considering mirror nuclei constraint. The rms deviation with respect to 2149 measured nuclear masses is reduced to 0.441 MeV. The shell corrections, the deformations of nuclei, the neutron and proton drip lines, and the shell gaps are also investigated to test the model. The rms deviation of α -decay energies of 46 super-heavy nuclei is reduced to 0.263 MeV. The central position of the super-heavy island could lie around $N = 176 \sim 178$ and $Z = 116 \sim 120$ according to the shell corrections of nuclei.

*Electronic address: wangning@gxnu.edu.cn

I. INTRODUCTION

The concept of symmetry in physics is a very powerful tool for understanding the behavior of Nature. The isospin symmetry discovered by Heisenberg plays an important role in nuclear physics. In the absence of Coulomb interactions between the protons, a perfectly charge-symmetric and charge-independent nuclear force would result in the binding energies of mirror nuclei (i.e. nuclei with the same atomic number A but with the proton number Z and neutron number N interchanged) being identical [1, 2]. Although the Coulomb interaction can result in the isospin-symmetry-breaking (ISB), the measured energy differences in the excited analogue states between mirror nuclei (MED) amount to tens of keV and do not generally exceed 100 keV, which indicates that the "nuclear part" of the binding energies in pairs of mirror nuclei should be close to each other, i.e.

$$E_B - E_C \approx E'_B - E'_C. \quad (1)$$

Where, E_B and E_C denote the total energy and the Coulomb energy of a nucleus, respectively, and E'_B and E'_C denote the corresponding values of the mirror nucleus. Combining the macroscopic-microscopic mass formula and Eq.(1), one can obtain the constraint between the shell corrections of the mirror nuclei,

$$|\Delta E - \Delta E'| \approx 0, \quad (2)$$

that is to say, a small value for the difference of the shell corrections of a nucleus and of its mirror nucleus. It is interesting to study the constraint between mirror nuclei and the ISB effect for improving the nuclear mass formula, especially for the calculations of neutron-rich nuclei and super-heavy nuclei.

In addition, the influence of the Coulomb interaction on the single-particle levels attracted a lot attention in recent years. It has been shown that single-particle effects, induced by the electromagnetic spin-orbit interaction and the Coulomb orbital term, produce large effects in the MED for nuclei in the upper sd and fp shells [3]. In [4], the authors found that the Coulomb potential strength does not change the position of magic gaps 50, 82 and 126, but strongly influences the shell structure of super-heavy nuclei. These investigations show that it is necessary to study the influence of the Coulomb term on the isospin-symmetry-breaking and on the binding energies of nuclei. The aim of the present work is to improve

the semi-empirical mass formula through studying the mirror nuclei constraint due to the isospin-symmetry and the influence of the Coulomb term on the single-particle levels and consequently on the shell corrections of nuclei. The paper is organized as follows: In Sec.II, we introduce the semi-empirical nuclear mass formula and some modifications in this work. In Sec. III, some results with the proposed model are presented. Finally, conclusions and discussions are contained in Sec.IV.

II. MODIFICATIONS OF THE MASS FORMULA

In [5], we proposed an semi-empirical nuclear mass formula based on the macroscopic-microscopic method [6]. The total energy of a nucleus can be calculated as a sum of the liquid-drop energy and the Strutinsky shell correction ΔE ,

$$E(A, Z, \beta) = E_{\text{LD}}(A, Z) \prod_{k \geq 2} (1 + b_k \beta_k^2) + \Delta E(A, Z, \beta). \quad (3)$$

The liquid drop energy of a spherical nucleus $E_{\text{LD}}(A, Z)$ is described by a modified Bethe-Weizsäcker mass formula,

$$E_{\text{LD}}(A, Z) = a_v A + a_s A^{2/3} + E_C + a_{\text{sym}} I^2 A + a_{\text{pair}} A^{-1/3} \delta_{np} \quad (4)$$

with isospin asymmetry $I = (N - Z)/A$, and the symmetry energy coefficient,

$$a_{\text{sym}} = c_{\text{sym}} \left[1 - \frac{\kappa}{A^{1/3}} + \frac{2 - |I|}{2 + |I|A} \right]. \quad (5)$$

The isospin dependence of the pairing term is also considered (see the expression of δ_{np} in [5] for details). The terms with b_k describe the contribution of nuclear deformation to the macroscopic energy, and the mass dependence of b_k is written as,

$$b_k = \left(\frac{k}{2} \right) g_1 A^{1/3} + \left(\frac{k}{2} \right)^2 g_2 A^{-1/3}. \quad (6)$$

The shell correction is obtained by the traditional Strutinsky procedure [7] by setting the order $p = 6$ of the Gauss-Hermite polynomials and the smoothing parameter $\gamma = 1.2\hbar\omega_0$ with $\hbar\omega_0 = 41A^{-1/3}$ MeV. For the deformation of nuclei, we only consider axially-deformed cases.

In this work, we make the following modifications to the mass formula:

- The Coulomb energy form is slightly changed, $Z(Z - 1)$ is replaced by Z^2 ,

$$E_C = a_c \frac{Z^2}{A^{1/3}} [1 - Z^{-2/3}] , \quad (7)$$

following the form in the finite range droplet model (FRDM) [6]. This modification can slightly improve the rms deviation with respect to 2149 measured nuclear masses [8] of nuclei [N and $Z \geq 8$] by about $2 \sim 3\%$.

- The microscopic shell correction of a nucleus is modified as,

$$\Delta E = c_1 E_{\text{sh}} + |I| E'_{\text{sh}}. \quad (8)$$

Where, E_{sh} and E'_{sh} denote the shell energy of a nucleus and of its mirror nucleus, respectively. The additionally introduced $|I| E'_{\text{sh}}$ term is to empirically take into account the mirror nuclei constraint and the isospin-symmetry-breaking effect. We find that this term can considerably reduce the rms deviation of masses by about 10%. The isospin-dependence in Eq.(8) is to consider the increase of the difference between neutron-neutron and proton-proton pairs in neutron-rich or proton-rich nuclei. The $|I| E'_{\text{sh}}$ term can effectively reduce the shell correction deviation $|\Delta E - \Delta E'|$ in pairs of mirror nuclei, which is required from the constraint in Eq.(2) and is helpful to restore the isospin symmetry in the mirror nuclei. If without the $|I| E'_{\text{sh}}$ term in Eq.(8), we obtain

$$|\Delta E - \Delta E'| = c_1 |E_{\text{sh}} - E'_{\text{sh}}|. \quad (9)$$

Considering the $|I| E'_{\text{sh}}$ term in ΔE , we obtain

$$\begin{aligned} |\Delta E - \Delta E'| &= (c_1 - |I|) |E_{\text{sh}} - E'_{\text{sh}}| \\ &\leq c_1 |E_{\text{sh}} - E'_{\text{sh}}|. \end{aligned} \quad (10)$$

To illustrate this point, in Fig.1(a) we show the values of $\Delta E' - \Delta E$ between mirror nuclei as a function of neutron number with the WS model [5]. The balls denote the experimental values of the nuclear energy difference $(E_B - E_C) - (E'_B - E'_C)$ between mirror nuclei by adopting the Coulomb energy form in the WS model. One can see that the experimental binding energies of pairs of mirror nuclei are indeed close to each other as mentioned previously when removing the Coulomb energies and the deviations

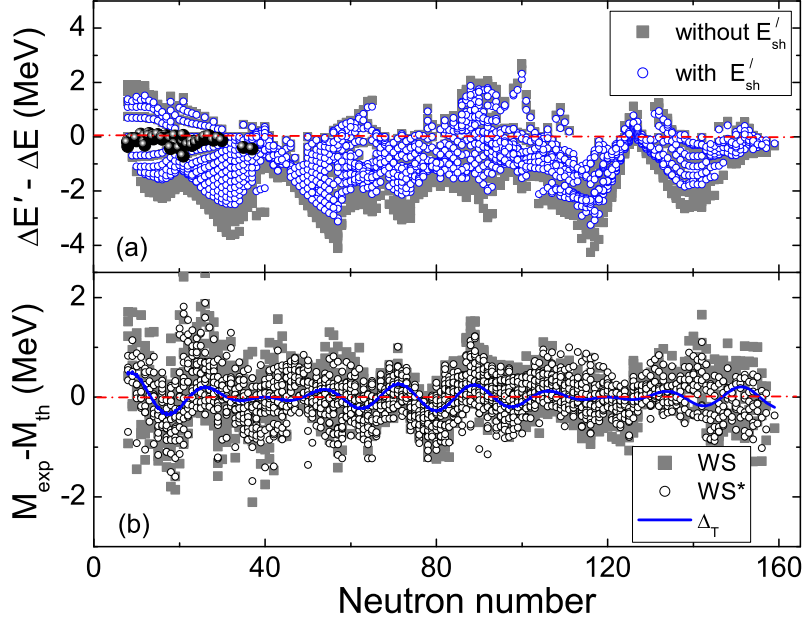


FIG. 1: (Color online) (a) Shell correction difference $\Delta E' - \Delta E$ in pairs of mirror nuclei. The squares and the open circles denote the results without and with the E'_{sh} term being taken into account, respectively. The balls denote the experimental values of $(E_B - E_C) - (E'_B - E'_C)$ between mirror nuclei with the Coulomb energy form in [5]. (b) Deviations of the calculated nuclear masses from the experimental data [8]. The squares and the crosses denote the results of WS and WS*, respectively. The solid curve denote the results of an empirical formula, $\Delta_T = -0.7 [\cos(2\pi \frac{N}{16}) + \cos(2\pi \frac{N}{20})] A^{-1/3}$, which will be discussed later.

are generally smaller than 1 MeV. The squares and the circles denote the results of shell correction difference without and with the $|I|E'_{sh}$ term being taken into account, respectively. Here, the shell energy of a nucleus is calculated at the deformation of its mirror nucleus for the sake of simplicity, since the deformations of pairs of mirror nuclei are close to each other for most nuclei according to the calculated results with WS. The WS calculations show that the shell correction differences caused by the Coulomb potentials are larger than 3 MeV for some mirror nuclei, which obviously over-predict the experimental nuclear energy differences [see the balls in Fig.1(a)]. The electromagnetic spin-orbit interaction, the Coulomb orbital term or the Coulomb

potential strength are therefore introduced by some authors [3, 4] for improving the traditional Coulomb potential as mentioned previously. In this work, the influence of the Coulomb term is effectively considered by introducing the shell energy of the mirror nuclei. The shell correction difference between mirror nuclei is effectively reduced by about 1 MeV after the $|I|E'_{\text{sh}}$ term being considered in ΔE .

- The β_6 deformation of nuclei is taken into account, which slightly improves the results of heavy nuclei.

III. RESULTS

With these modifications and the obtained optimal parameters of mass formula which are listed in Table 1 and labelled as WS*, the rms deviations of the 2149 nuclear masses is further reduced by 15%, to 0.441 MeV and the rms deviations of the neutron separation energies of 1988 nuclei is reduced to 0.332 MeV (see Table 2). Fig.1 (b) shows the deviations of the calculated nuclear masses from the experimental data. Considering the shell constraint between mirror nuclei (WS*), the results are effectively improved.

In Fig.2 we show the calculated shell corrections ΔE of nuclei with this model. Considering the shell constraint between mirror nuclei, the nuclei with the largest shell corrections in the super-heavy region slightly moves to $N = 176$ and $Z = 120$. The shell energies with WS* for nuclei around $N = 16$ and $N = 28$ become larger in absolute values, whilst those for nuclei around $(N = 184, Z = 82)$ and ^{100}Sn become smaller compared with the WS calculations. In Fig.3, we show the calculated deformations of nuclei with WS*. Obviously, the calculated structure of the known magic nuclei is spherical in shape. For light nuclei, the β_6 deformations of nuclei are not very obvious, compared with the intermediate and heavy nuclei. In Fig.4, we show the deviations of the calculated nuclear masses in this work from the results of other models as a function of isospin asymmetry. One can see that for highly neutron-rich nuclei ($I > 0.3$) the deviations from these different models are large, and the results from FRDM and WS* are relatively close to each other, while the results from WS are relatively close to those of HFB-17 [10].

In Fig.5, we show the drip lines obtained with different mass formulas. To remove the fluctuations due to the shell and pairing effects, we do a polynomial fitting to the calculated results with the FRDM, the HFB-17, and the WS* models, respectively. The leftmost and

TABLE I: Model parameters of the mass formula.

parameter	WS	WS*
a_v (MeV)	-15.5841	-15.6223
a_s (MeV)	18.2359	18.0571
a_c (MeV)	0.7173	0.7194
c_{sym} (MeV)	29.2876	29.1563
κ	1.4492	1.3484
a_{pair} (MeV)	-5.5108	-5.4423
g_1	0.00862	0.00895
g_2	-0.4730	-0.4632
c_1	0.7274	0.6297
V_0 (MeV)	-47.4784	-46.8784
r_0 (fm)	1.3840	1.3840
a (fm)	0.7842	0.7842
λ_0	26.3163	26.3163

TABLE II: rms σ deviations between data AME2003 [8] and predictions of several models (in MeV). The line $\sigma(M)$ refers to all the 2149 measured masses, the line $\sigma(S_n)$ to the 1988 measured neutron separation energies S_n . The calculated masses with FRDM are taken from [6]. The masses with HFB-14 and HFB-17 are taken from [9] and [10], respectively. WS*+ Δ_T means the correction Δ_T for empirically considering the tetrahedral deformation is added to the binding energy of a nucleus with WS*.

	FRDM	HFB-14	HFB-17	WS	WS*	WS*+ Δ_T
$\sigma(M)$	0.656	0.729	0.581	0.516	0.441	0.417
$\sigma(S_n)$	0.399	0.598	0.506	0.346	0.332	0.330

rightmost curves denote the smooth proton drip line (for odd-Z nuclei) and the smooth neutron drip line, respectively. The crosses denote the measured nuclei. For the proton drip line, the three models give similar results. For the neutron drip line, the results slightly deviate from each other at heavy mass region. Based on the liquid-drop model, the neutron separation energy of an intermediate and heavy nucleus ($A \gg 1$) can be approximately

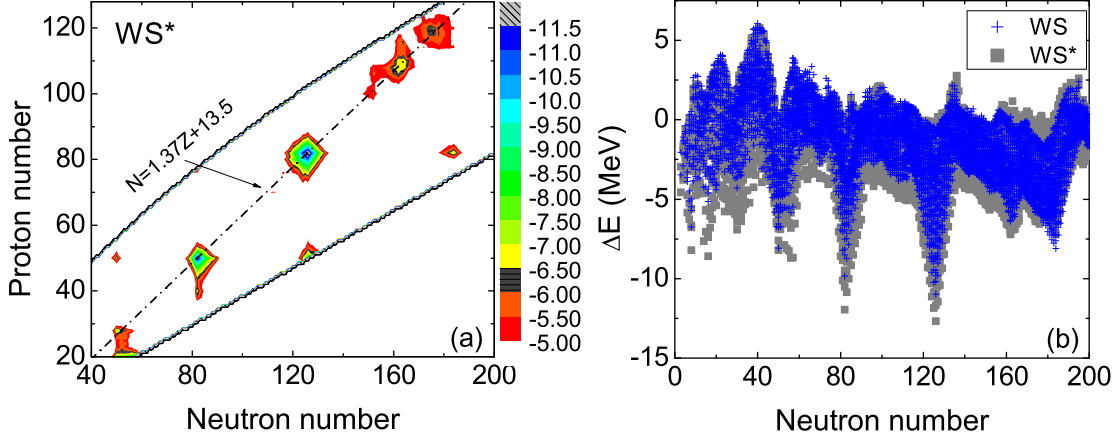


FIG. 2: (Color online) (a) Contour plot of shell corrections of nuclei with WS*. The dot-dashed line passes through the areas with the known heavy magic nuclei. (b) Shell corrections of nuclei as a function of neutron number. The crosses and the squares denote the results of WS and WS*, respectively.

written as,

$$S_n \simeq -a_v - 2a_{\text{sym}}I. \quad (11)$$

Where, a_v (negative value) and a_{sym} (positive value) are the coefficients of the volume energy and the symmetry energy of a nucleus, respectively. For the neutron drip line ($S_n = 0$) of intermediate and heavy mass region, we obtain the isospin asymmetry at the drip line

$$I_{nd} \simeq -\frac{1}{2} \frac{a_v}{a_{\text{sym}}}. \quad (12)$$

One can see that the neutron drip line directly relates to the ratio of a_v to a_{sym} . The difference of the neutron drip line from different models is probably due to the difference of the coefficients a_v and a_{sym} adopted in the models. For nuclei with $A \rightarrow \infty$ or asymmetric nuclear matter ($a_v \approx -16$ MeV and $a_{\text{sym}} \approx 32$ MeV), we obtain the corresponding neutron drip line which is also shown in Fig.5 (solid-squared line). From the figure, one can see that most of measured nuclei are located in the left side of the solid-squared line. In addition, we show the smooth β -stability line from FRDM (open-squared curve) and WS* (solid-circled

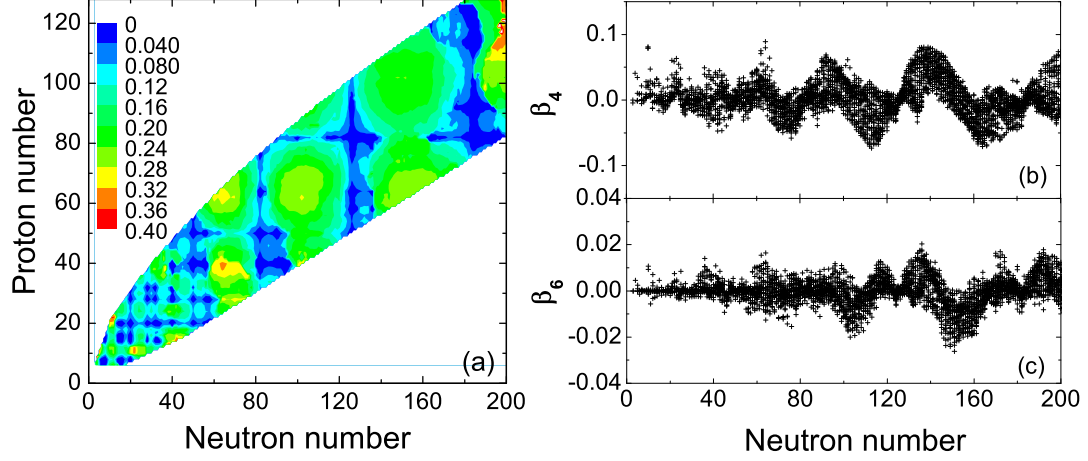


FIG. 3: (Color online) (a) Contour plot of quadrupole deformation $|\beta_2|$ of nuclei with WS*. (b) β_4 and (c) β_6 of nuclei as a function of neutron number, respectively.

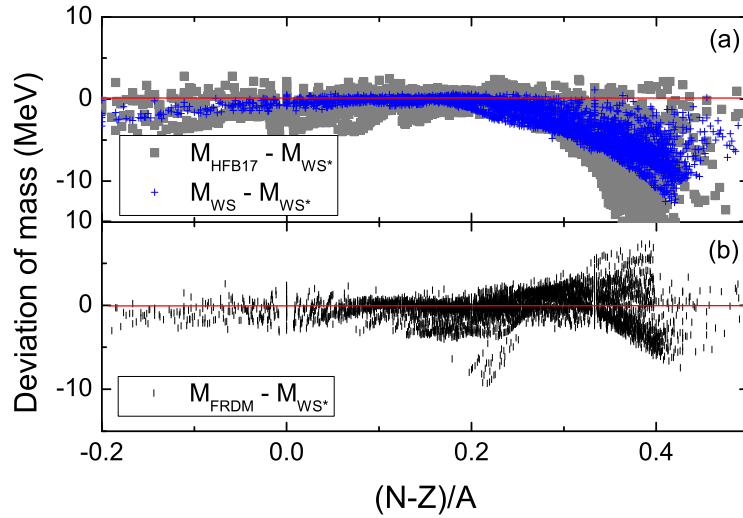


FIG. 4: (Color online) Deviations of calculated nuclear masses in this work from the results of other models. The calculated masses with FRDM and HFB-17 are taken from [6] and [10], respectively.

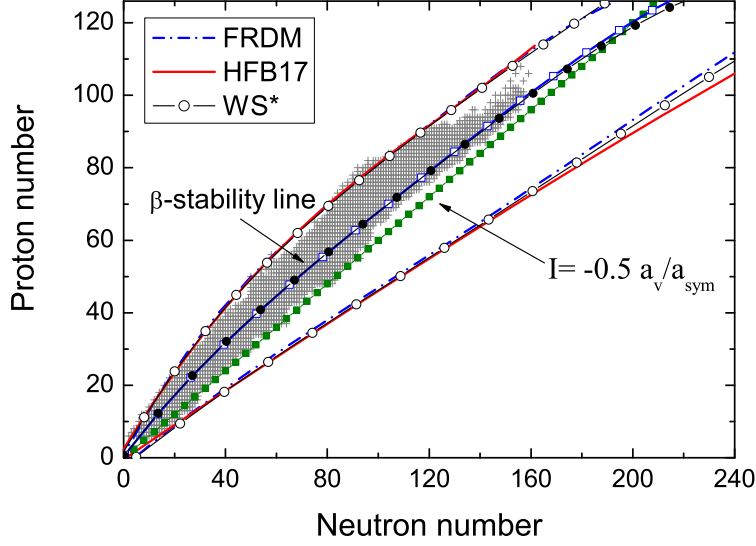


FIG. 5: (Color online) Smooth drip lines from different mass formulas. The crosses denote the measured nuclei. The solid-squared line denote the neutron drip line of nuclei $A \rightarrow \infty$ with $I = -\frac{1}{2} \frac{a_v}{a_{\text{sym}}}$ and taking $a_v = -16$ MeV and $a_{\text{sym}} = 32$ MeV. The open-squared and the solid-circled curve denote the smooth β -stability line from FRDM and WS* calculations, respectively.

curve) calculations, respectively. At $Z = 120$, the corresponding neutron number of the nuclei along the β -stability line is about $N = 200$.

To further test the model, we study the shell gaps. As a measure of the discontinuity in the two neutron separation energy S_{2n} at magic neutron numbers N_0 , the shell gap [11],

$$\Delta_n(N_0, Z) = S_{2n}(N_0, Z) - S_{2n}(N_0 + 2, Z), \quad (13)$$

is a sensitive quantity to test the model. In Fig.6, we show the calculated shell gaps at the magic neutron numbers $N_0 = 28, 50, 82, 126$ with different models. The dashed, the dot-dashed and the solid curve denote the results of HFB-17, FRDM and WS*, respectively. The squared curve denote the experimental data. The most shell gaps can be reasonable well described by the WS* model, except the shell gap at sub-shell closure $Z = 64$ which is over-predicted by WS* and FRDM and is under-predicted by the HFB-17 model. In Fig.6(b), the peak (large shell gap) at magic number $Z = 28$ disappears according to the HFB-17 calculations, and the peak at $Z = 82$ can not be reasonably well described from the

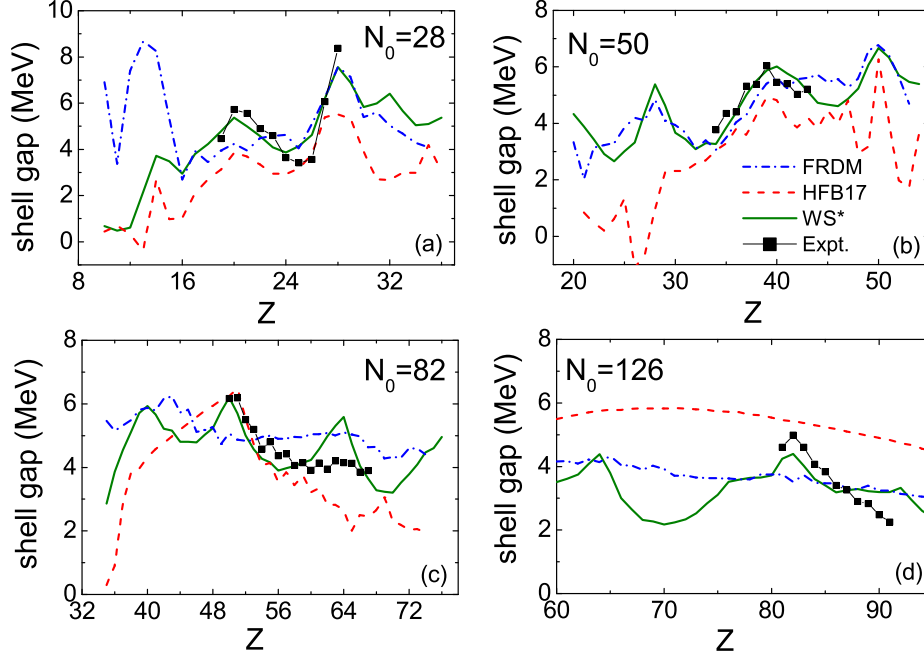


FIG. 6: (Color online) Shell gap calculated with different models. The dashed, the dot-dashed and the solid curve denote the results of HFB-17, FRDM and WS*, respectively. The squared curve denote the experimental data.

FRDM and HFB-17 calculations in Fig.6(d). The experimental shell gaps at magic numbers $Z = 20, 28, 40, 50, 82$ can be remarkably well described with the proposed model.

In addition, we study the relation between the fission barrier of super-heavy nucleus and the corresponding shell correction of the nucleus. Neglecting the shell energy at the saddle point, the fission barrier of a nucleus can be approximately written as [12],

$$B_f \approx B_{LD} - \Delta E. \quad (14)$$

Where B_{LD} and ΔE are the macroscopic fission barrier and the shell correction of a nucleus at its ground state. For super-heavy nucleus, the macroscopic fission barrier generally disappears and consequently the fission barrier can be roughly evaluated through the corresponding shell correction of the nucleus. In Fig.7, we show the fission barriers of a number of super-heavy nuclei (solid-circled curve) [13] which are calculated with the macroscopic-microscopic approach, considering the deformation of system up to β_8 and the triaxial deformation. The open-circled curve and the crosses denote the values of $-\Delta E$ with WS and

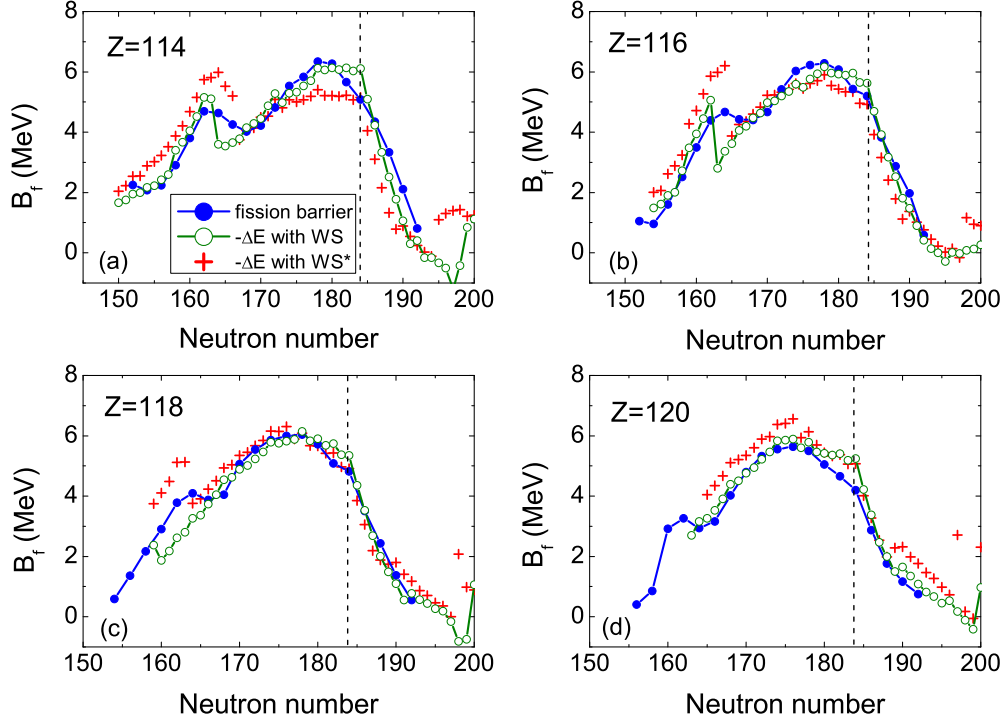


FIG. 7: (Color online) Fission barriers of some super-heavy nuclei. The solid-circled curve denote the calculated fission barriers of super-heavy nuclei in Ref.[13]. The open-circled curve and the crosses denote the values of $-\Delta E$ with WS and WS*, respectively. The dashed line denotes the position $N = 184$.

WS*, respectively. One can see that the calculated fission barriers are generally close to the values of $-\Delta E$ with WS. Both of models in which the mirror nuclei constraint is not taken into account, predict the two neutron magic numbers $N = 162$ and $N = 178$ at the super-heavy region. When the constraint between mirror nuclei is considered (WS*), the results for nuclei with $Z = 116$ and 118 do not change too much around $N = 178$, while the results for nuclei with $Z = 114$ and 120 change about 1 MeV. These investigations indicate: 1) The calculated shell corrections (in absolute value) with the proposed mass formula are comparable to the fission barriers of super-heavy nuclei; 2) The mirror nuclei constraint could influence the shell structure of nuclei with $Z = 114$ and 120 . In Fig.7, the dashed lines denotes the position $N = 184$. For nuclei with $N > 184$, the fission barriers fall rapidly with the increase of neutron number. In addition, the shell corrections (in absolute value) of

TABLE III: α -decay energies Q_α and the shell corrections in 6 α -decay chains with WS* (in MeV). The experimental data are taken from [14, 15].

A	Z	$Q_\alpha(\text{Expt.})$	$Q_\alpha(\text{WS}^*)$	$\Delta E(\text{WS}^*)$	A	Z	$Q_\alpha(\text{Expt.})$	$Q_\alpha(\text{WS}^*)$	$\Delta E(\text{WS}^*)$
294	117	10.96(10)	11.32	-5.77	293	117	11.18(8)	11.62	-5.70
290	115	10.09(40)	10.38	-5.17	289	115	10.45(9)	10.34	-5.28
286	113	9.77(10)	9.82	-4.33	285	113	9.88(9)	10.13	-4.46
282	111	9.13(10)	9.62	-4.10	281	111	-	10.04	-4.17
278	109	9.69(19)	9.66	-4.88	277	109	-	9.75	-5.07
274	107	8.93(10)	8.71	-4.80	273	107	-	8.98	-5.05
296	120	-	13.25	-6.56	298	120	-	12.81	-6.13
292	118	-	12.06	-6.16	294	118	11.81(6)	12.15	-6.31
288	116	-	11.31	-5.32	290	116	11.00(8)	11.12	-5.61
284	114	-	10.93	-4.50	286	114	10.33(6)	10.25	-5.09
280	112	-	10.90	-4.51	282	112	-	10.27	-4.68
304	120	-	12.49	-5.08	320	120	-	9.85	-2.31
300	118	-	11.70	-5.43	316	118	-	9.27	-2.08
296	116	-	10.98	-5.43	312	116	-	8.73	-0.14
292	114	-	9.12	-5.40	298	114	-	8.07	-5.15
288	112	-	9.36	-4.46	294	112	-	8.38	-3.77

nuclei with $Z > 120$ are obviously smaller than that of $^{292}\text{120}$. According to the calculated shell corrections of nuclei, the central position of the super-heavy island could lie around $N = 176 \sim 178$ and $Z = 116 \sim 120$.

Furthermore, we study the α -decay energies of 46 super-heavy nuclei (the experimental data are taken from Ref. [14], Table I of Ref.[15] and Table II of Ref.[16]). The rms deviation of the α -decay energies of the 46 super-heavy nuclei falls from 0.566 MeV with FRDM to 0.263 MeV with the WS* model (the corresponding result with WS is 0.284 MeV). In Table III, we list the α -decay energies Q_α and the shell corrections ΔE in 6 α -decay chains of super-heavy nuclei with $Z = 117$ [14] and $Z = 120$. The available experimental data can be reproduced reasonably well. These calculations indicate that the proposed mass formula is relatively reliable for description of the masses of super-heavy nuclei.

IV. CONCLUSION AND DISCUSSION

In summary, the semi-empirical mass formula based on the macroscopic-microscopic method has been further improved by considering the constraint between mirror nuclei. The rms deviation with respect to 2149 measured nuclear masses is reduced to 0.441 MeV and the rms deviation of the neutron separation energies of 1988 nuclei falls to 0.332 MeV. The shell corrections, the deformations of nuclei and the neutron and proton drip lines have been investigated also. The predicted central position of the super-heavy island according to the calculated shell corrections of nuclei could lie around $N = 176 \sim 178$ and $Z = 116 \sim 120$, considering the mirror nuclei constraint. The shell corrections of super-heavy nuclei (in absolute value) are close to the corresponding fission barriers of the nuclei from other macroscopic-microscopic model. The shell gaps at proton magic numbers $Z = 20, 28, 40, 50, 82$ can be remarkably well described with the proposed model. The rms deviation of the α -decay energies of 46 super-heavy nuclei is reduced from 0.566 MeV with FRDM to 0.263 MeV with the proposed model in this work.

In addition, we note that the deviations from the measured masses for some nuclei with $N \approx 18, 26, 40, 56, 64, 70, 80, 88$ etc. are relatively large, with both WS and WS*, which may be caused by the triaxial deformation of nuclei or the tetrahedral symmetry in nuclei [17, 18]. It is found that the strongest tetrahedral-symmetry effects appear at tetrahedral-magic numbers 16, 20, 32, 40, 56, etc., and the tetrahedral deformation can bring over a few MeV of energy gain in the nucleus [18]. We empirically describe the influence of the tetrahedral deformation on the binding energies of nuclei by using two cosine functions together with the two tetrahedral-magic numbers 16 and 20, $\Delta_T = -0.7 [\cos(2\pi\frac{N}{16}) + \cos(2\pi\frac{N}{20})] A^{-1/3}$ MeV. The solid curve in Fig.1 (b) denotes the results of Δ_T . With the empirical function Δ_T , the rms deviation of 2149 nuclear masses can be further reduced by 5%, to 0.417 MeV. Microscopic study on the triaxial deformation of nuclei is in progress.

ACKNOWLEDGEMENTS

We thank Prof. Zhuxia Li and Prof. Xiaohong Zhou for valuable suggestions. This work was supported by National Natural Science Foundation of China, Nos 10875031, 10847004 and 10865002. The obtained mass table with the proposed formula is available from <http://www.imqmd.com/wangning/WS3.3.zip>.

-
- [1] S. M. Lenzi and M. A. Bentley, *Lecture Notes in Physics*, **764**, 57 (2009).
 - [2] S. Shlomo, *Rep. Prog. Phys.* **41**, 957 (1978)
 - [3] S. M. Lenzi, *J. Phys.: Conf. Seri.* **49**, 85 (2006).
 - [4] S. Ćwiok, J. Dobaczewski, et al., *Nucl. Phys. A* **611**, 211 (1996).
 - [5] Ning Wang, Min Liu and Xizhen Wu, *Phys. Rev. C* **81**, 044322 (2010).
 - [6] P. Möller, J. R. Nix, et al., *At. Data and Nucl. Data Tables* **59**, 185 (1995).
 - [7] V. M. Strutinsky and F. A. Ivanjuk, *Nucl. Phys. A* **255**, 405 (1975).
 - [8] G. Audi, A.H. Wapstra and C. Thibault, *Nucl. Phys. A* **729**, 337 (2003).
 - [9] S. Goriely, M. Samyn and J. M. Pearson, *Phys. Rev. C* **75**, 064312 (2007).
 - [10] S. Goriely, N. Chamel and J. M. Pearson, *Phys. Rev. Lett.* **102**, 152503 (2009).
 - [11] D. Lunney, J.M. Pearson, C. Thibault, *Rev. Mod. Phys.* **75**, 1021 (2003).
 - [12] Ning Wang, et al., *Phys. Rev. C* **77**, 014603 (2008).
 - [13] M. Kowal, P. Jachimowicz and A. Sobiczewski, *Phys. Rev. C* **82**, 014303 (2010).
 - [14] Yu. Ts. Oganessian et al., *Phys. Rev. Lett.* **104**, 142502 (2010).
 - [15] Jianmin Dong, Wei Zuo, et al., *Phys. Rev. C* **81**, 064309 (2010), and references therein.
 - [16] Di-Da Zhang, Zhong-Yu Ma, et al., *Phys. Rev. C* **81**, 044319 (2010), and references therein.
 - [17] D. Curien, J. Dudek and K. Mazurek, *J. Phys.: Conf. Seri.* **205**, 012034 (2010).
 - [18] J. Dudek, et al., *Phys. Rev. Lett.* **88**, 252502 (2002).